ACOUSTIC EMISSION APPLICATION TO THE SINGLE SPECIMEN DETERMINATION OF J_{IC} FOR STEELS

V. DAL RE*

The Acoustic Emission technique can discriminate the damage mechanism in progress inside the material by the counts, amplitudes and their statistical distribution measurement. A single specimen technique for the J_{IC} determination of some steels is discussed. The onset of subcritical crack extension is detected by a simultaneous sudden rise of the counts/s and peak-amplitude curves and by a fall of the amplitude distribution slope. The results obtained in some steels by this technique and by the classic four specimens method have been compared and have shown to be in good agreement.

INTRODUCTION

The direct measurement of fracture toughness (K_{IC}) for steels (1),(2),sometimes needs very thick specimens (up to 125-150 mm) and therefore very high loads.

The must widley used test method for the indirect K_{IC} measurement using relatively small specimens, is that proposed by Landes and Begley (3).

This method needs the making, pre-cracking, loading, heat-tinting of almost four specimens for each test.

Several test methods have been developped to attain the J_{IC} measurement with a single specimen (4),(5),(6),(7),(8),(9). The results obtained by the acoustic emission technique in several steels are presented; their comparison with the results obtained by the Landes and Begley's method (3) and by the direct K_{IC} measurement (1),(2) shows to be in good agreement.

It is intuitive that the acoustic emission technique, whose characteristics (amplitude and counts) are strictly connected with the damage mechanisms of material, can detect in a sharply cracked specimen, the onset of subcritical crack extension after previous plastic deformation during crack-tip blunting.

METHODOLOGY

The acoustic emission detection has been performed during the J_{IC} measurement according to ASTM STP 514 (3).

The acoustic emission instrumentation was a Dunegan-Endevco mod.3000

* Associate Professor. University of Bologna. Italy.

whose block-diagram is shown in Fig.1. Two S 9204 acoustic emission piezoelectric transducers (sensitivity 65 dB ref. 1 Volt per meter per second) were applied to the specimen.

By the use of the locate function and the "spatial window" it is possible to exclude the acoustic emission signals not coming from the crack-zone in peak-amplitude analysis. Acoustic emissions generated by pin rotation and by plastic deformation of the holes are neglected.

In order to minimize the acoustic noise caused by pin contact stress, all specimens were preloaded, before notching, to levels well above those expected in the test (Kaiser effect). (9)

The ground noise caused by the hydraulic test machine (Instron mod. 8033) has been eliminated by two "mechanical attenuators" (Fig.2) based on acoustic emission reflection in different attenuation materials.

A typical location of the acoustic emission events is shown in Fig.3, where the higher emissivity zone corresponding to the crack-tip is evident.

The acoustic emission detection was restricted to the central part of the specimen. Loads, counts/s, peak-amplitude and slope were plotted versus displacement by a four channels recorder.

ACOUSTIC EMISSION PARAMETRS

In order to detect the onset of the subcritical crack extension after the first crack-tip plastic deformation, three acoustic emission parameters have been considered:

a) Counts b) Peak-amplitude c) Slope of statistical distribution in the cumulative form.

a) Count-rate. It is known that acoustic emissions detected during plastic deformation of a steel are characterized by a quasi-continuous count-rate with small peak-amplitude, whereas crack propagations are characterized by a sudden energy release with a sharp count-rate increase. This measurement is the easiest to obtain and only needs a counter and a reset-clock.

b) Peak-amplitude. Also the peak-amplitude record shows a sudden increase at the onset of the first subcritical crack extension. This measurement needs an amplitude detector.

c) Slope of amplitude statistical distribution in the cumulative form. In this representation the acoustic emission events are classified, according to their peak-amplitude, in 101 fields from 0 to 100 dB, and for each field the corresponding number of events is recorded. The amplitude histogram can be represented in the normal or in the cumulative form (Fig.4)

The slope of the latter curve is typical of each specific phenomenon within the material (10) and can be continuously recorded during the test. At the start of the loading of the specimen, acoustic emission events are characterized by small amplitude values and the slope of the curve is high. When also high amplitude events begin to take place, typical of crack-extension, the slope of the curve suddenly falls. The contemporaneous onset of phenomena described in a),b),c) denotes with good accuracy the first crack-extension.

The value of J is calculated as a function of displacement from the

expression: $$J = \frac{2A}{B(W-a)}$$ where:

A is the area under the load-displacement curve, taken at the displacement of interest;

B is the thickness of the specimen;

W-a is the uncracked ligament (Fig.5).

With this method, the critical value of J, named J_{IC}, is taken when acoustic emission detection shows the first subcritical crack propagation. The corresponding K_{IC} value is calculated by the well known expression:

$$K_{IC} = \sqrt{\frac{J_{IC} E}{1-\nu^2}} \qquad (1)$$

EXPERIMENTAL RESULTS

The tested materials are:

"A"- Steel UNI 28NiCrMoV12 normalized
"B"- " UNI 28NiCrMoV12 in H.A.Z.
"C"- " UNI 28NiCrMoV12 in weld bead
"D"- " UNI 18NiCrMo5 oil-hardened
"E"- " UNI 20MnCr5 "

The chemical compositions of the steels investigated are presented in Table 1

Table 1. Chemical composition of the steelsinvestigated

Material	C	Ni	Cr	Mo	V	Mn	Pb	S	Al	Si	P
28NiCrMoV12	.26	2.80	1.60	.55	.13	-	-	-	-	-	-
18NiCrMo5	.18	1.30	.80	.20	-	.82	.15	.034	.043	.285	.006
20MnCr5	.23	.26	1.24	.03	-	1.34	-	.005	.032	.23	.01

All tests were performed at room-temperature of 20°C. The experimental results obtained are presented in Table 2.

A comparison of experimental results obtained shows to be in good agreement.

The values of J_{IC} and K_{IC} obtained by acoustic emissions are always somewhat lower than those obtained by ASTM STP 514 method, as obtained by other authors in different steels. (9)

The appearance of characteristic acoustic emission diagrams plotted during these tests is affected by the different toughnesses of the steels and consequently by the different acoustic emissivity.

Table 2. Experimental results

Material	J_{IC} ASTM STP514 kJ/m^2	J_{IC} A.E. kJ/m^2	K_{IC} A.E. expr.(1) $MN/m^{3/2}$	K_{IC} /1/,/2/ $MN/m^{3/2}$
"A"	255	249	237	-
"B"	215	213.7	220	-
"C"	56	55	111	-
"D"	32.2	30	82	88
"E"	26.9	26.2	77	77.4

A much higher emissivity occurs in brittle steels ("D", "E") than in more ductile steels ("A", "B", "C").

The different total gains employed in different cases are presented in Table 3.

Table 3. Gain values

Material	"A"	"B"	"C"	"D"	"E"
Gain dB	86	86	84	76	76

The plots of acoustic emission parameters regarding the steel "A" are shown in Fig.6. The first onset of crack propagation is located by the first sudden peak in the counts/s curve and by the contemporaneous fall in the slope curve. The following counts/s peaks and the falls of the slope show the next steps of crack-growth.

In this case the peak-amplitude was not plotted.

The J-resistance-curve of steel "A" obtained by four specimen method (3), is shown in Fig.7.

The plots of acoustic emission parameters regarding the steel "B" are shown in Fig.8. The interpretation of these plots is similar to the previous one.

The J-resistance-curve of steel "B" is presented in Fig.9.

In the plots of acoustic emission parameters of steel "C", (Fig.10), the first peak of counts/s, corresponding to J_{IC}=39.9kJ/m^2, has been neglected because it is not accompanied by a significant fall of the slope and by an amplitude peak, typical of the first crack-growth.

The J-resistance-curve of steel "C" is shown in Fig.11.

Because of higher brittleness of steel "D", the counts/s plot (Fig.12) has a more irregular behaviour; but also in this case the onset of crack-growth is marked by a high counts/s peak accompanied by a contemporaneous fall of the slope.

The J-resistance-curve of steel "D" is shown in Fig.13.

The acoustic emission plots and the J-resistance-curve regarding the steel "E" (Fig.14 and 15) have a similar behaviour because of the similarity of these steels.

For steels "D" and "E" valid direct K_{IC} tests (1), (2), have been performed on 1TCT specimens (thickness 25 mm) and the results obtained were:

Material "D": K_{IC} = 88 MN/m$^{3/2}$

Material "E": K_{IC} = 77.4 MN/m$^{3/2}$

For a correct set-up of the acoustic emission intrumentation, some good information on the emissivity of each steel has been obtained during pre-cracking of the specimen.

CONCLUSIONS

The acoustic emission technique results in supplying valid help to the J_{IC} measurement because it can detect the onset of stable crack-growth, also with only a single specimen.

A complete acoustic emission instrumentation, able to detect counts/s, peak-amplitude and statistical distribution, and energy, is useful for a correct and unambiguous measurement, nevertheless a more simple instrumentation,

only able to detect counts and count-rate, is sufficient to obtain quite accurate measurements.

All J_{IC} values obtained by this method are always lower than those measured according to ASTM STP 514 procedure; the difference is always between 0.6% and 6.8% and therefore is in good agreement.

ACKNOWLEDGEMENTS

This research was partly financed by C.N.R. (National Research Council): Contribution CT 80.01121.07.

REFERENCES

1. "Standard Method of Test for Plane-Strain Fracture Toughness of Metallic Materials", (ASTM E399-74).

2. "Method for Plane-Strain Fracture Toughness (K_{IC}) Testing", British Standard 5447, (1977).

3. Begley J.A., and Landes J.D., "Fracture Toughness", ASTM STP 514.

4. Landes J.D., and Begley J.A., "Recent Developments in Fracture Mechanics Test Methods Standardisation", ASTM STP632-77.

5. Lereim L., and Embury J.D., "A Simple Method for the Determination of J-Integral Values", Engineering Fracture Mechanics, 11, (1979) 161.

6. Okumura N., "Application of the AC Potential Drop Technique to the Determination of R-Curves of Tough Ferritic Steels", Engineering Fracture Mechanics, 14, (1981) 617.

7. Tseng M.K., Marcus H.L.: "A Single Specimen Determination of J_{IC} for Alluminium Alloys", Engineering Fracture Mechanics, 16, (1982) 895.

8. Lai Z.H., Chen L.J., Chang C.M., Ma C.S., and Chao C.S., "A New Method of Determining J_{IC} of Steel by Means of Single Specimen", Engineering Fracture Mechanics, 17, (1983) 395.

9. Takahashi H., Khan M.A., Kikuchi M., and Suzuki M., "Acoustic Emission Crack Monitoring in Fracture Toughness Tests for AISI and SA 533B Steels", Experimental Mechanics, March (1981) 89.

10. Lenain J.C., "L'analyse statistique dans l'émission acoustique", Revue Pratique de Contrôle Industriel, 45bis.

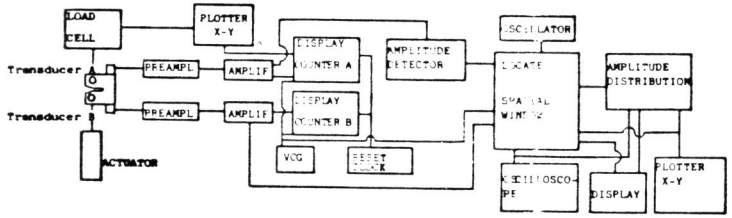

Fig. 1. Block Diagram of Acoustic Emission Instrumentation

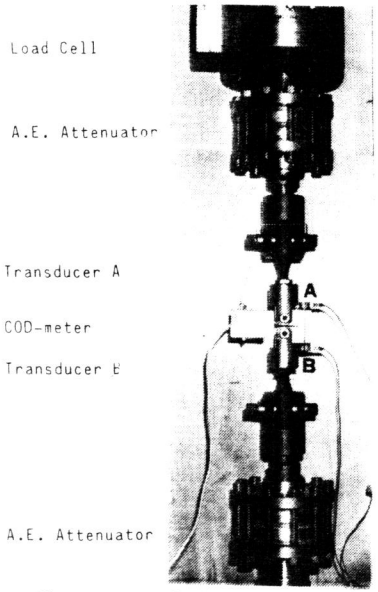

Fig. 2. General View of the Load Equipment

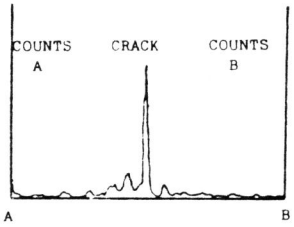

Fig. 3. Typical Locate Distribution

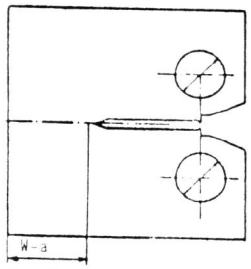

Fig. 5. The J_{IC} Specimen

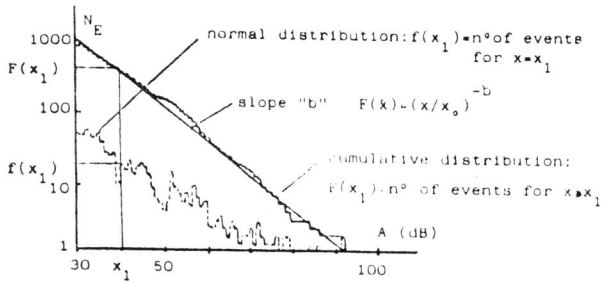

Fig. 4. Amplitude Statistical Distribution

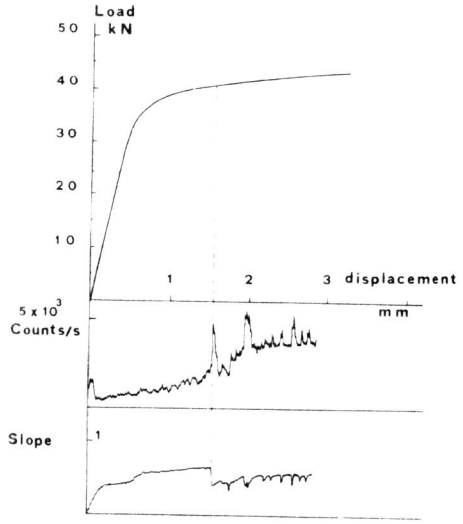

Fig. 6. Acoustic Emission Plots. Material "A"

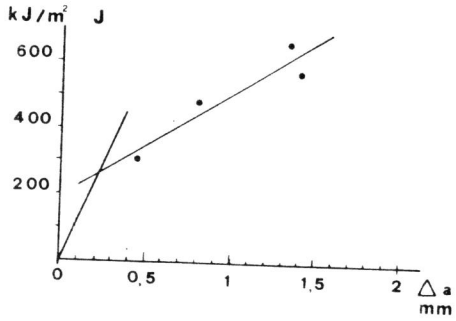

Fig. 7. J-Resistance Curve. Material "A"

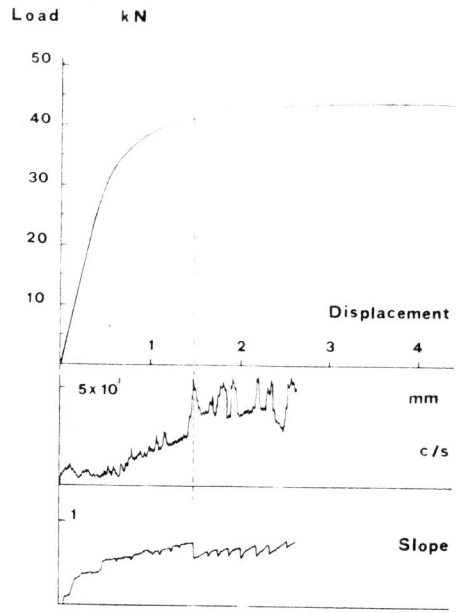

Fig. 8. Acoustic Emission Plots. Material "B"

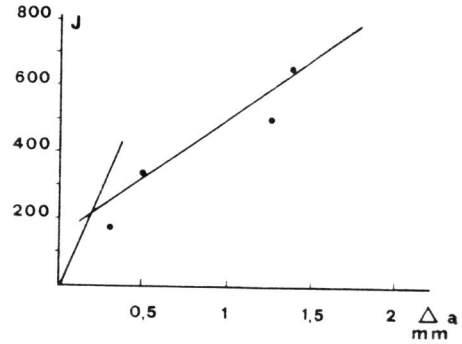

Fig. 9. J-Resistance Curve. Material "B"

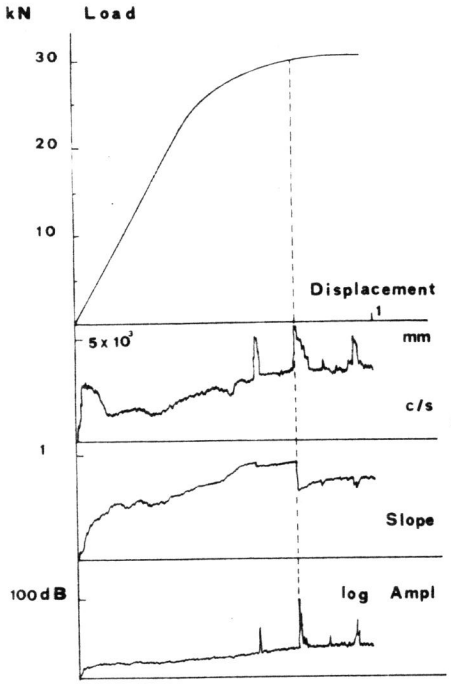

Fig. 10. Acoustic Emission Plots.
Material "C"

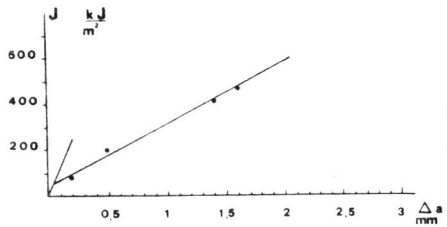

Fig. 11. J-Resistance Curve
Material "C"

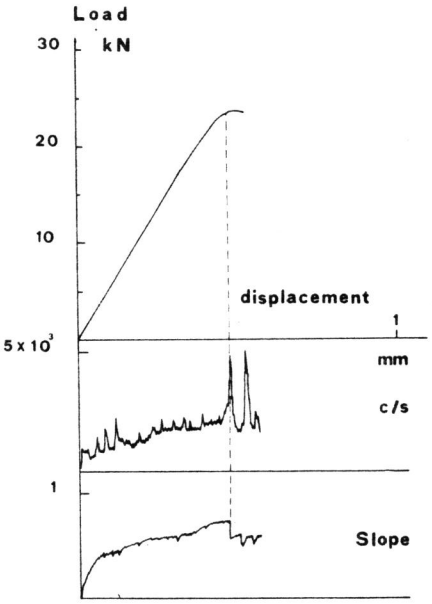

Fig. 12. Acoustic Emission Plots.
Material "D"

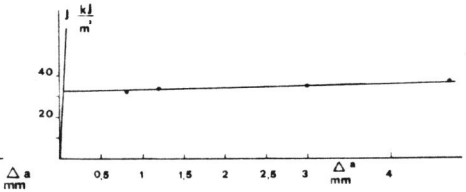

Fig. 13. J-Resistance Curve
Material "D"

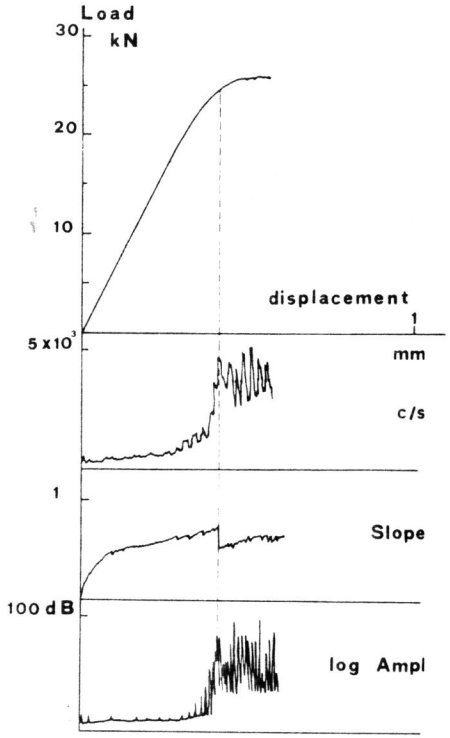

Fig. 14. Acoustic Emission Plots.
Material "E"

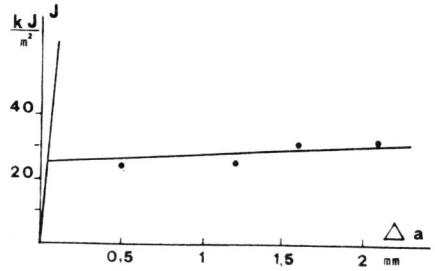

Fig. 15. J-Resistance curve.
Material "E"